Configurational Statistics of Poly(dimethylsiloxane). 2. A New Rotational Isomeric State Approach

Ivet Bahar

Department of Chemical Engineering and Polymer Research Center, Bogazici University, Bebek 80815, Istanbul, Turkey

Ignacio Zuniga

Departamento de Fisica Fundamental, UNED, Apartado 60141, 28080 Madrid, Spain

Robert Dodge and Wayne L. Mattice*

Institute of Polymer Science, University of Akron, Akron, Ohio 44325-3909

ABSTRACT: A new rotational isomeric state treatment, compatible with the molecular mechanics and dynamics considerations of the preceding paper, is introduced for describing the conformational statistics of poly(dimethylsiloxane). In view of the smooth distribution of rotamers deduced from molecular dynamics simulations, softer potentials are assigned to bonds in gauche states compared to the model of Flory, Crescenzi, and Mark. Second-order interactions prevailing in states involving trans bonds are included in the theory. The model yields satisfactory agreement with experiments on the mean-square unperturbed end-to-end separations, the mean-square dipole moment and its temperature dependence, and the molar cyclization equilibrium constants for dimethylsiloxane oligomers. It cannot account for the positive temperature coefficient of the unperturbed chain dimensions. Intramolecular interactions extending beyond first and second neighbors along the chan are investigated as a possible origin of the discrepancy.

I. Introduction

From the molecular mechanics and dynamics analysis carried out in the preceding paper,[1] a rather smooth energy distribution of isomeric configurations is predicted for poly(dimethylsiloxane) (PDMS). Accordingly, backbone bonds in PDMS may assume almost any rotation without substantial preference for any of them. Even the unfavorable intramolecular interactions that may possibly arise in specific compact configurations are found to be easily alleviated by suitable distortion of the chain geometry. As a result, consecutive bond torsions leading to rotamers that may be identified with the g^+g^- or g^-g^+ states occur to an appreciable extent. In light of this picture, it is not possible to rationalize the energy parameters adopted by Flory, Crescenzi, and Mark[2,3] (FCM) in their statistical treatment of PDMS. Those parameters were originally derived from the analysis of the unperturbed dimensions of the chain in methyl ethyl ketone, under Θ conditions (at 343 K) and were later adopted for the theoretical analysis of the chains in different media or in the bulk state. The FCM model satisfactorily explained the experimentally measured unperturbed dimensions[4] and their temperature dependence[5] but seriously fails in interpreting the cyclization equilibria of oligomeric chains of $x = 4$–11 units.[6-9] The purpose of the present work is to determine a new set of parameters that will be compatible with the fundamental energetics and molecular dynamics considerations, on the one hand, and that will satisfactorily reproduce experimental findings, on the other.

A rotational isomeric state (RIS) formalism based on pairwise interdependence of skeletal bonds will be adopted in the statistical treatment of PDMS, in agreement with previous work.[3] Three rotational states defined by the torsional angles 180° (trans, t), 60° (gauche⁻, g⁻), and 300° (gauche⁺, g⁺) will be assumed for each backbone bond. The adoption of three equally spaced rotational states is justifiable only as a convenient mathematical device. However, the definition of a given rotational isomeric state needs revision in the sense that a given state t, g⁺, or g⁻

is now representative of a rather broad range of torsional angles, each extending over one-third of the complete cycle of 360°.

In the following section the RIS formalism applicable to PDMS and the related matrix generation approach are briefly presented. The molecular dynamics simulation of ref 1 reveals the distinct behavior of the two types of bond pairs (O–Si, Si–O) and (Si–O, O–Si), insofar as the secondary intramolecular interactions dominant in the tt state are concerned. Accordingly, a new energy parameter accounting for this feature will be incorporated into the statistical treatment. In the third section, the applications of the RIS formalism will be presented and compared with experiments. Attention will be focused on two major subjects concerning (i) the unperturbed dimensions of the chain and (ii) the cyclization equilibrium of oligomers. The former includes the mean-square end-to-end distance, $\langle r^2 \rangle_0$, resulting from viscometric measurements under Θ conditions,[4] its temperature coefficient d ln $\langle r^2 \rangle_0$/dT obtained from stress-temperature behavior,[5] and the mean-square dipole moments $\langle \mu^2 \rangle_0$, from dielectric relaxation experiments.[10] As to the second subject, the experimental data are furnished by the equilibrium constants K_x associated with the cyclization reactions of dimethylsiloxane oligomers.[6-9] That the equilibrium constants are directly proportional to the probability of occurrence of cyclic conformers follows from the theory of Jacobson and Stockmayer.[11,12] K_x values are sensitive to the precise distribution of configurations and provide a relatively critical test of the validity of a given statistical model.

The probability distribution curves depicted in Figures 6–8 of the preceding manuscript furnish information on the pairwise interdependent behavior of skeletal bonds. As presented above, they may be readily used to deduce representative first- and second-order interaction parameters controlling the chain statistics, on the premises that a Markov chain model is applicable to PDMS. Calculations performed below will demonstrate that a model chain of *independent* bonds cannot account for the equilibrium properties of PDMS, no matter what the choice for first-

order interactions is, but a RIS approach based on *pairwise interdependent* bonds satisfactorily reproduces isothermal measurements related to unperturbed chain dimensions and cyclization equilibrium. Yet, that approach is insufficient to yield the experimentally measured temperature coefficient. A critical examination of the coupling of adjacent bond rotations will be carried out in the Discussion and Conclusion section, using both molecular mechanics and MD simulations to assess the role and importance of longer range correlations between skeletal bonds.

II. Statistical Theory

A. Statistical Weights and Configurational Partition Function. On the basis of the probability distribution curves resulting from molecular dynamics simulations, two statistical weight matrices of the form

$$\mathbf{U}_a = \begin{bmatrix} \tau & \sigma & \sigma \\ 1 & \sigma\psi & \sigma\omega \\ 1 & \sigma\omega & \sigma\psi \end{bmatrix} \tag{1}$$

and

$$\mathbf{U}_b = \begin{bmatrix} \tau' & \sigma & \sigma \\ 1 & \sigma\psi' & \sigma\omega' \\ 1 & \sigma\omega' & \sigma\psi' \end{bmatrix} \tag{2}$$

will be adopted for the pair of bonds (O–Si, Si–O) and (Si–O, O–Si), respectively. Here σ is the statistical weight parameter associated with the first-order interaction energy E_σ of gauche bonds relative to trans bonds. This statistical weight is identical for the two skeletal bonds Si–O and O–Si, inasmuch as the atoms separated by three bonds are the same in both cases. However, second-order interactions, prevailing between atoms separated by four bonds, depend on the pair of bonds under consideration. The statistical weights corresponding to the pair of bonds (Si–O, O–Si) are indicated by the primed variables to distinguish them from those of the pair (O–Si, Si–O). Here τ (or τ') accounts for the contribution of the second-order interactions E_τ (or $E_{\tau'}$) taking place in the tt state, provided that those of the $tg^\pm$ or $g^\pm t$ are chosen as reference. Similarly, ω and ψ refer to the second-order interactions associated with the $g^\mp g^\pm$ and $g^\pm g^\pm$ states and are related to the corresponding energies E_ω (or $E_{\omega'}$) and E_ψ (or $E_{\psi'}$), in the same way as the other parameters, by the Boltzmann equalities

$$\sigma = \exp(-E_\sigma/RT)$$

$$\tau = \exp(-E_\tau/RT)$$

$$\omega = \exp(-E_\omega/RT)$$

$$\psi = \exp(-E_\psi/RT) \tag{3}$$

Clearly, the same relationships hold for the primed quantities. Serial multiplication of statistical weight matrices yields the configurational partition function, Z, according to[3]

$$Z = \mathbf{U}_1[\mathbf{U}_a \quad \mathbf{U}_b]^{x-1}\mathbf{U}_n \tag{4}$$

where

$$\mathbf{U}_1 \equiv [1 \quad 0 \quad 0] \tag{5}$$

and

$$\mathbf{U}_n \equiv \text{col} (1 \quad 1 \quad 1) \tag{6}$$

B. Square of the Magnitude of the Chain Vector. The mean-square end-to-end distance $\langle r^2 \rangle_0$ may be calculated by serial multiplication of generator supermatrices as[13]

$$\langle r^2 \rangle_0 = Z^{-1}\mathscr{G}_{[1}[\mathscr{G}_a \quad \mathscr{G}_b]^{x-1}\mathscr{G}_{n]} \tag{7}$$

Here the generator supermatrices are given by

$$\mathscr{G}_{[1} = \mathbf{U}_1 \otimes \mathbf{G}_{[1} \tag{8}$$

$$\mathscr{G}_{n]} = \mathbf{U}_n \otimes \mathbf{G}_{n]} \tag{9}$$

$$\mathscr{G} = (\mathbf{U}_i \otimes \mathbf{E}_5)\|\mathbf{G}_i\|, \quad i = a \text{ or } b \tag{10}$$

where $\mathbf{E}_5$ is the identity matrix of order 5, $\otimes$ indicates the direct product, and the matrices $\mathbf{G}_{[1}$ and $\mathbf{G}_{n]}$ are, respectively, the first row and the last column of the 5 × 5 generator matrix

$$\mathbf{G}_i = \begin{bmatrix} 1 & 2\mathbf{I}^T\mathbf{T} & I^2 \\ 0 & \mathbf{T} & \mathbf{I} \\ 0 & 0 & 1 \end{bmatrix} \tag{11}$$

for bond i. $\mathbf{T}_i$ in eq 11 is the conventional transformation matrix expressing vectorial or tensorial quantities of the bond-based frame $i + 1$, in terms of their representations in frame i.[3,13] It is a function of the dihedral angle ϕ_i for bond i and the bond angle θ_i between bonds i and $i + 1$. $\mathbf{I}_i$ is the ith bond vector along the chain. Its magnitude is denoted by I. The superscript T indicates the transpose of a vector. In PDMS, $\mathbf{T}_i$ is a function of either $\theta_a = 110°$ or $\theta_b = 143°$ depending on the index i. $\mathbf{I}_i$ assumes the form col (1.63 0 0) for all i. The double bar matrix $\|\mathbf{G}_i\|$ in eq 10 is the diagonal supermatrix of the form

$$\|\mathbf{G}_i\| = \begin{bmatrix} \mathbf{G}_i(\phi_i=180°) & & \\ & \mathbf{G}_i(\phi_i=300°) & \\ & & \mathbf{G}_i(\phi_i=60°) \end{bmatrix} \tag{12}$$

The subscript i is replaced by a or b for bonds Si–O and O–Si, respectively. The set of eqs 7–12 constitutes a computationally efficient tool to evaluate $\langle r^2 \rangle_0$. The same method may be used for the computation of $\langle \mu^2 \rangle_0$, provided that $\mathbf{I}_i$ in eq 11 is replaced by $\mathbf{I}_a = \text{col} (\mu_0 \ 0 \ 0)$ and $\mathbf{I}_b = \text{col} (-\mu_0 \ 0 \ 0)$, depending on the type of skeletal bond. Here μ_0 is the magnitude of the dipole moment vector connecting atoms Si and O and is taken as 0.6 D.[8]

C. Cyclization Equilibrium. Following the Jacobson and Stockmayer theory, the molar cyclization equilibrium constant K_x for the ring-chain equilibrates is directly proportional to the concentration of cyclic compounds. In the limit of high extents of reaction, K_x is given by[11,14]

$$K_x = \bar{W}_x/2N_A x \tag{13}$$

where K_x is expressed in moles per liter, N_A is Avogadro's number, and $\bar{W}_x$ is the density of cyclic chains. $\bar{W}_x$ is given by

$$\bar{W}_x = [3/2\pi\langle r_x^2 \rangle_0]^{3/2} \tag{14}$$

for the case $\mathbf{r} = 0$, provided that a Gaussian distribution of end-to-end vectors $\mathbf{r}$ applies. Here $\langle r_x^2 \rangle_0$ represents the mean-square end-to-end distance of chains consisting

of x monomeric units. Using the equality

$$C_n = \langle r_x^2 \rangle_0 / (2xl^2) \tag{15}$$

for the characteristic ratio C_n of a chain of $n = 2x$ skeletal bonds, each of length l, and substituting eq 14 into eq 13, the molar cyclization constant equates to[3,7]

$$K_x = \frac{[3/\pi]^{3/2}}{2^4 l^3 C_n^{3/2} x^{5/2} N_A} \tag{16}$$

Alternatively, a more rigorous expression for the density of cyclic chains, which avoids any averaging of the distribution of chain vectors, is the complete enumeration or direct computational method based on the relationship[7-9]

$$\bar{W}_x = [(4/3)\pi r^3]^{-1} z_r / Z_c \tag{17}$$

for chains whose terminal atoms are separated by a distance less than or equal to r. Here z_r is the total statistical weights of the conformers satisfying the requirement $|\mathbf{r}| \leq r$, where $|\mathbf{r}|$ is the magnitude of the end-to-end vector $\mathbf{r}$. For the particular case of cyclic dimethylsiloxanes of the form $[(CH_3)_2SiO]_x$, the partition function Z_c in eq 17 reads

$$Z_c = U_1[U_a \ U_b]^{x-2} U_a U_n \tag{18}$$

which differs from eq 4 due to the lack of the terminal (Si–O, O–Si) bond pair. The subscript c is appended to the partition function employed in the cyclization equilibrium to distinguish it from the one corresponding to the noncyclic chain, Z. Z_c comprises the sum of the statistical weights of a set of 3^{2x-3} conformations, bearing in mind that the rotations of the terminal bonds are immaterial, in prescribing r. The latter should be considered in cases where the orientation of the terminal bonds is of considerable importance, as carried out in the theory developed by Flory, Suter, and Mutter.[15] No directional restriction is considered in the present study, in parallel to the previous treatment by Semlyen and collaborators.[7-9]

The FCM model was shown to yield K_x values far lower than those found experimentally in the range $x = 4$–6[7] and too high for $x > 10$.[8] Agreement between theory and experiment was achieved only by according a statistical weight equal to 22 (instead of zero) to any pair of bonds (O–Si, Si–O) in state g^+g^- or g^-g^+ surrounded by gauche bonds of opposite sign and preceded by a trans bond to form the sequence $tg^+g^-g^+g^-$ or $tg^-g^+g^-g^+$. It is clear that this statistical weight is not compatible at all with the FCM model in which the tt state is assigned the largest weight (eq 1), and the g^+g^- or g^-g^+ states are exclusively precluded for the pair of bonds (O–Si, Si–O). Nevertheless, this modification was applied to the range $4 \leq x \leq 6$ only, and no theoretical model applicable throughout a wide range of chain length has been proposed so far. The present work is an attempt in this direction.

III. Calculations and Comparison with Experiments

A. Unperturbed Chain Dimensions and Mean-Square Dipole Moments. In view of the high flexibility of the chain and the availability of a wide variety of rotameric states without strong preference for any of them, a freely rotating chain model may seem justifiable as a first approximation for PDMS. However, the values for the experimental characteristic ratios and dipole moments turn out to be well above those of freely rotating chains. It is thus clear that such a simple model is not applicable and it is necessary to consider restrictions in bond rotations due to intramolecular conformational potentials.
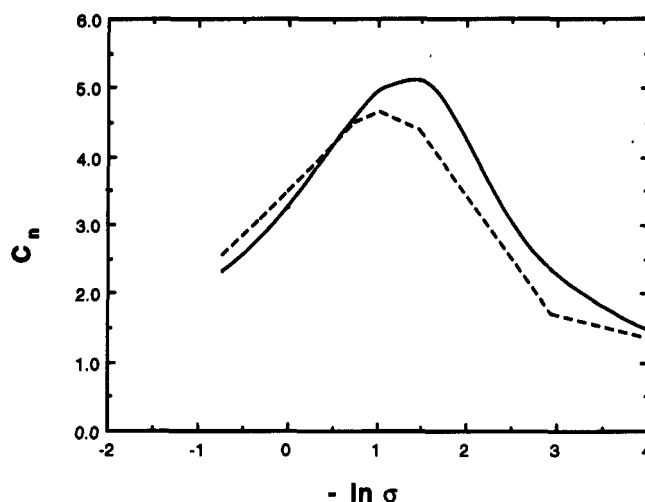
Figure 1. Dependence of the characteristic ratio on $-\ln \sigma$, for PDMS model chains with independent bonds. The solid and dashed curves are calculated for $\theta_b = 143°$ and $150°$, respectively. Three equally spaced rotameric states t, g^+, and g^- with respective torsional angles $180°$, $300°$, and $60°$ are assumed, as in all calculations.
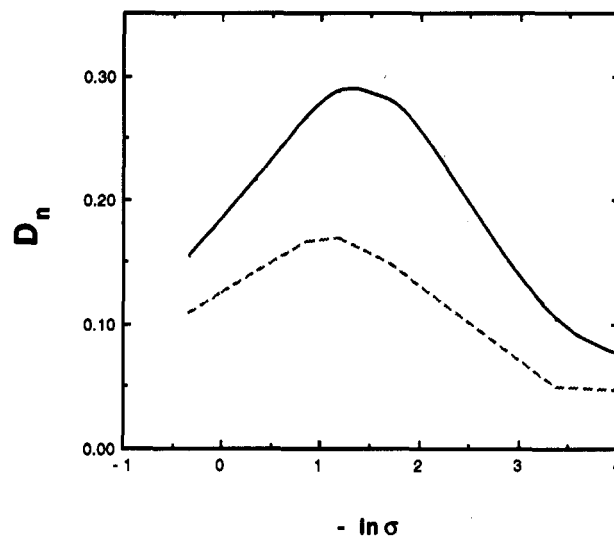
Figure 2. Dependence of the dipole ratio on $-\ln \sigma$, for PDMS model chains with independent bonds. The solid and dashed curves are calculated for $\theta_b = 143°$ and $150°$, respectively.

With the addition of independent rotational potentials operating on skeletal bonds, a single parameter σ characterizes the difference in conformational energy between trans and gauche states. The inadequacy of such a model becomes clear upon examination of Figures 1 and 2. They depict the dependence of the characteristic ratio C_n and the dipole ratio

$$D_n = \langle \mu^2 \rangle_0 / n\mu_0^2 \tag{19}$$

where μ_0 is the dipole of a Si–O bond, on the parameter σ, for a PDMS chain of $n = 100$ independent bonds. The two variables C_n and D_n can not attain their respective experimental values of about 6.3 and 0.33, irrespective of the choice of σ. The curves in Figures 1 and 2 are obtained by using the geometry parameters $l_{Si-O} = 1.63$ Å, $\theta_a = 110°$, and $\phi_i = 180°$, $300°$, and $60°$ for the t, g^+ and g^- states, respectively. Results for $\theta_b = 143°$, adopted in the FCM model, and $\theta_b = 150°$, used by Grigoras and Lane,[16] are shown by the solid and dashed curves, respectively, in each figure, to assess the influence of the relatively smooth bond bending potential on the mean dimensions of the chain. It should be pointed out that the characteristic ratio of about 6.3 is obtained from viscosity measurements
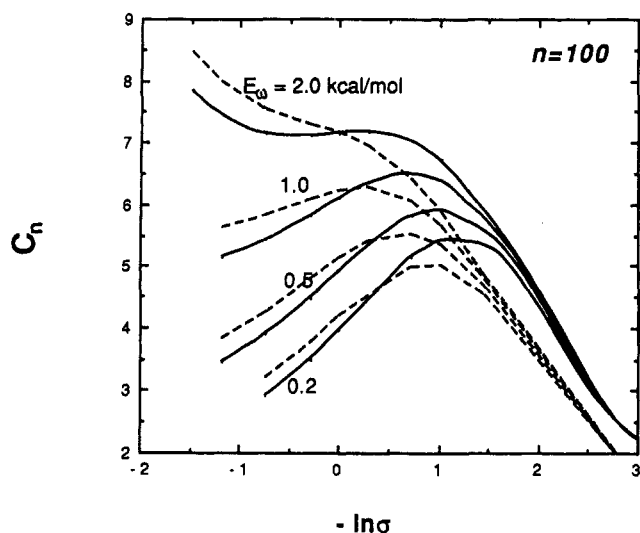
Figure 3. Influence of ω on C_n. All second-order interactions are neglected, except for E_ω, which is taken as the indicated values, on each curve (the same for both skeletal bonds). The solid and dashed curves are calculated for $\theta_b = 143°$ and $150°$, respectively.

Table I
Energy Parameters (kcal/mol)

param α	energy $(E_\alpha)^a$	$E_\alpha{}^b$	$E_\alpha{}^c$
σ	0.20	0.85	0.30
τ	0.37	0.00	0.35
τ'	0.02	0.00	-0.10
ω	0.45	∞	0.60
ω'	0.04	1.05	0.35
ψ	0.12	0.00	0.25
ψ'	0.06	0.00	0.20

^{a} From molecular dynamics analysis of ref 1. ^{b} From the FCM model.[2] ^{c} Present work.

in solvents with cohesive energy exceeding that of the polymer and C_n is further increased in solvents with lower cohesive energy density.

Figures 1 and 2 indicate that the characteristic ratio and dipole moment of PDMS cannot be accounted for by first-order interactions alone. Higher order interdependence between skeletal bonds should be incorporated into the treatment. For an understanding of the role of secondary interactions on C_n, exploratory calculations have been performed by assuming $\tau = \tau' = \psi = \psi' = 1$ and $\omega = \omega'$ and modifying the second-order interaction parameter ω. The parameter ω is expected to be of significant importance in describing the statistical behavior of the chain. The resulting C_n vs $-\ln \sigma$ curves are displayed in Figure 3 for various choices of ω. The curves are found to shift upward, as required, by inclusion of secondary interactions. The same trend is observed in dipole ratios as well. This figure illustrates the necessity of introducing higher order interaction parameters into the theory, for a reasonable agreement with experiment.

The molecular mechanics and dynamic analysis carried out in the preceding paper give insights into the types and reasonable ranges of intramolecular conformational energy prevailing in PDMS. Energy parameters deduced from the above considerations are listed in the second column of Table I. For comparative purposes, those of the FCM model are given in the third column of the table. Although those values satisfactorily reproduce experimental $\langle r^2 \rangle_0$ and $\langle \mu^2 \rangle_0$, they cannot be rationalized on the basis of simple energetic/probabilistic considerations, as shown above. Exploratory calculations using energy parameters compatible with those of column 2 lead to the set of parameters presented in the fourth column of Table I, which yields
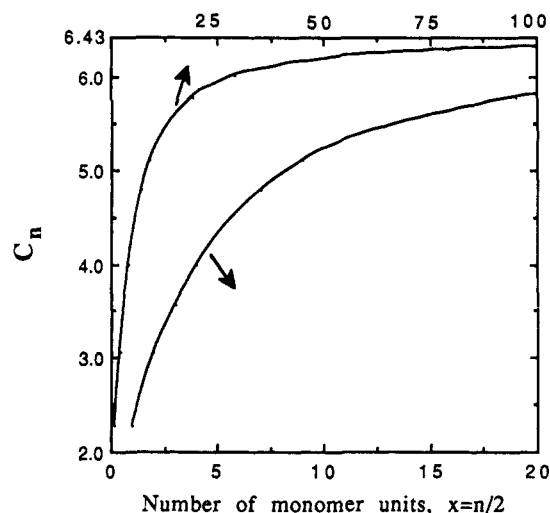
Figure 4. Dependence of C_n on $x = n/2$, at $T = 343$ K. The RIS scheme described in section II has been used with the energy parameters listed in the last column of Table I. The abscissa scales for the two curves are indicated by the arrows. The curves are almost indistinguishable from those obtained by Flory and Semlyen,[14] using the FCM model.[2]
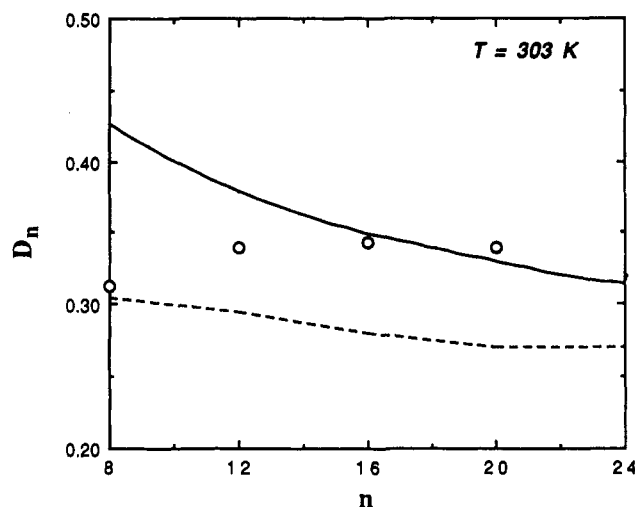
Figure 5. Dependence of D_n on n at $T = 303$ K. The dots are the experimental results from Sutton and Mark.[10] The solid curve results from the present model. The lower dashed curve is drawn from previous calculations[10] using the FCM model.

$\langle r^2 \rangle_0$ and $\langle \mu^2 \rangle_0$ values at least as satisfactory as the FCM model.

The change in the characteristic ratio with the size of the chain is displayed in Figure 4. The curves are calculated on the basis of the newly introduced parameters listed in the last column of Table I, for PDMS chains $CH_3[Si(CH_3)_2O]_{n/2}Si(CH_3)_3$ at 343 K. The two curves refer to the abscissa scales shown on the lower and upper margins, as indicated by the arrows. They are almost indistinguishable from those obtained by Flory and Semlyen,[3,14] using the energy parameters listed in column 3 of Table I. The same geometrical parameters are adopted in both approaches. It is noted that, for the chain terminated by Si atoms at both ends, the definitions of the matrices U_a and U_b are interchanged in the formulations presented above. Nevertheless, it is found by repeating calculations that the change in C_n is negligibly small for the case of hydroxy-terminated chains. The asymptotic limit $C_\infty = 6.43$ in Figure 4 is identical with that of Flory and Semlyen.[14]

The dependence of D_n on the number n of skeletal bonds between the terminal Si atoms is shown in Figure 5, for oligomers of various size. The dots represent the exper-
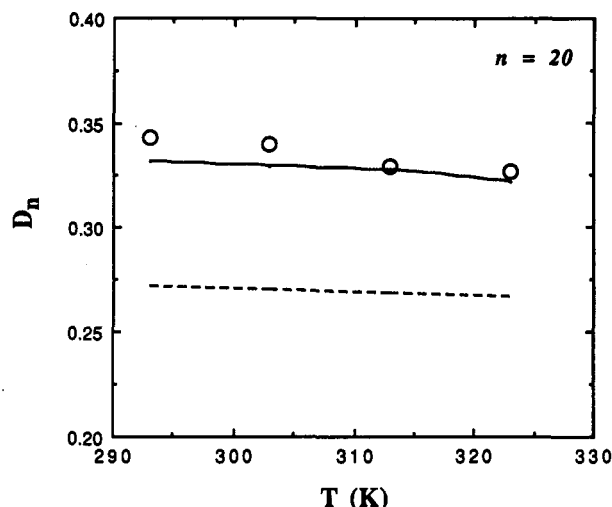
Figure 6. Temperature dependence of D_n for $n = 20$. The dots are the experimental results from Sutton and Mark.[10] The solid curve results from the present model. The lower dashed curve is drawn from previous calculations[10] using the FCM model.

Figure 7. Change in the molar cyclization constant K_x with x, for $[(CH_3)_2SiO]_x$. The open circles are the experimental results from Brown and Slusarczuk.[6] They are connected by a curve to guide the eye. The open triangles follow from the complete enumeration approach (eqs 13 and 17) using the FCM model. The filled circles are found by using the same approach, but with the present model. The dashed curve is found from eq 16, using the present model.

imental measurements by Sutton and Mark, at 303 K. The solid line is theoretically obtained using the energy parameters introduced in the last column of Table I. The dashed curve follows from the theoretical results reported by Sutton and Mark,[10] employing the FCM model. The asymptotic limit of the experimental curve is estimated[10] to be about 0.33, at 25 °C. The present theoretical approach yields a value of 0.25, whereas the FCM model leads[10] to 0.23. From those comparisons, the newly introduced energy parameters seem to adequately describe PDMS conformational statistics.

Insofar as the temperature dependence of the unperturbed dimensions is concerned, the new set of energy parameters does not compare favorably with experiments. In fact, the new RIS model fails to reproduce the positive temperature coefficient of about 0.7×10^{-3}/deg, for d ln $\langle r^2 \rangle_0/dT$, calculated both from precise measurements of stress-temperature coefficients in cross-linked networks and from the change in the intrinsic viscosity of athermal solutions with temperature. Although some deviations exist between the measurements by different groups, they all find a positive temperature coefficient. The present approach yields a coefficient of about -2.34×10^{-4}. A negative temperature coefficient is theoretically predicted for the dipole ratio as well. The latter is in satisfactory agreement with experiment, as may be observed from Figure 6. In the figure, experimental measurements for the oligomer with $n = 20$ are shown by the dots, as a function of temperature throughout the range of measurements. The present theoretical model yields the solid curve, which is found to conform closely to the experimental behavior. For illustrative purposes, the prediction of the FCM model is displayed by the dashed curve.

From the present analysis, it is observed that, except for the temperature coefficient d ln $\langle r^2 \rangle_0/dT$, quantities related to the unperturbed chain dimensions are well accounted for by the new set of energy parameters. The origin of the discrepancy between theory and experiment for the temperature coefficient is not clarified at this point. The influence of intramolecular interactions extending beyond first and second neighbors along the chain will be considered and discussed below as a possible explanation for the insufficiency of the present model to accurately reproduce d ln $\langle r^2 \rangle_0/dT$.

B. Cyclization Equilibria. As delineated above, evaluation of the molar cyclization constant K_x for various compounds of the form $[(CH_3)_2SiO]_x$ necessitates the de-

termination of the density of cyclic structures $\bar{W}_x$. The density of cyclic structures may be found either by an approximate method as in eq 14 or by a rigorous procedure based on the complete enumeration and weighting of all cyclic conformers contributing to z_r in eq 17. Previous studies indicate that the former approach satisfactorily reproduces experimental data, provided that x exceeds ~ 15. For shorter oligomers eq 14 is no longer applicable. A complete enumeration approach is necessary, and this approach has been previously undertaken.[7-9]

Figure 7 displays the results from experiments (empty circles) by Brown and Slusarczuk[6] in an equilibrate in toluene solution at 383 K. The dashed curve follows from the Gaussian approximation given by eq 16, in which the characteristic ratios evaluated by the present approach have been inserted. For illustrative purposes, the theoretical values found from the complete enumeration of cyclic oligomers weighted according to the FCM model are shown by the empty triangles in the figure. Those results are obtained by adopting $r = 3$ Å as the critical separation between chain ends to form a cyclic structure. The discrepancy of several orders of magnitude between theory and experiment, at low x values in particular, is clearly apparent. Also, the theoretical results are sensitive to the choice of critical r for cyclization. They are further depressed upon adoption of smaller r values, which points out the inadequacy of the FCM model to interpret the measurements.

The presently introduced RIS scheme with the energy parameters described above leads to the filled circles in the figure, in much better agreement with experiments. The results are calculated for $r = 1.25$ Å, which is a comparatively severe requirement to be fulfilled. Table II lists the details of the calculations for each x for the case $r = 1.25$ Å. In Table II z_r/Z_c is the probability of occurrence of this subset of cyclic conformers, $\bar{W}_x$ is the density in molecules per liter, and K_x is the equilibrium constant. Calculations carried out with the adoption of $r = 3.0$ Å as the upper critical separation for cyclization are found to

Table II
Probabilities and Densities of Cyclic Conformers with
$r = 1.25$ Å

value of x in $[(CH_3)_2SiO]_x$	no. of cyclic conformers	$z_r/Z_c \times 10^4$	$\bar{W}_x \times 10^2$ [a]	$\log K_x$ [b]
4	2	7.072	8.644	−1.746
5	12	5.094	6.226	−1.986
6	26	5.158	6.305	−2.059
7	370	4.972	6.077	−2.142
8	2248	5.695	6.960	−2.141
9	17392	2.923	3.575	−2.482
10	133062	1.634	1.997	−2.780
11	1060818	4.342	5.307	−2.397

[a] In molecules/L. [b] K_x in mol/L.

lead to K_x and/or $\bar{W}_x$ values of comparable magnitude. This is due to the mutual counterbalancing effects of (i) an increase in the population of configurations contributing to z_r and (ii) an increase in the volume element $4\pi r^3$, as may be observed from eq 17. The relative insensitivity of K_x values to the choice of r is a feature favoring the present computation scheme.

The satisfactory agreement between the predictions of the present theory and cyclization experiments, which is particularly remarkable in the range $6 < x < 11$, lends support to the adoption of the new model. The only point that is not reproducible is the temperature dependence of $\langle r^2 \rangle_0$. The possible origins of the limitations and insufficiency of the model in explaining the positive temperature coefficient will be presented in the next section.

IV. Discussion and Conclusion

A new RIS formalism has been introduced in the present work, which incorporates second-order interactions in addition to first-order potentials, distinguishing tt bonds from tg$^\pm$ or g$^\pm$t bonds, and employs energy parameters compatible with the molecular dynamics considerations of the preceding paper. The theory satisfactorily reproduces experimental $\langle r^2 \rangle_0$, $\langle \mu^2 \rangle_0$, the temperature dependence of mean dipole moments, and the molar cyclization equilibrium constants K_x for various size oligomers. However, the positive temperature coefficient d ln $\langle r^2 \rangle_0$/dT cannot be accounted for by the theory.

There are several approximations present in the RIS scheme adopted in the present study, which may be responsible for the deviation between theory and experiment as far as the temperature dependence of $\langle r^2 \rangle_0$ is concerned. Three equally spaced isomeric states are adopted in the treatment, whereas a rather smooth distribution of rotational angles allowing for substantial distortion of the chain geometry from those idealized torsional angles is observed from the MD trajectory. The present approach is based on a pairwise interdependence of skeletal bonds along the chain, while interactions extending beyond first and second neighbors may play a significant role in prescribing the conformational statistics of PDMS. The passage from *independent* to *pairwise interdependent* bonds is definitely required to correctly predict $\langle r^2 \rangle_0$ and $\langle \mu^2 \rangle_0$. In the absence of secondary interactions, regardless of the choice of a representative first-order parameter, no possible combination is found to attain those mean values. It is interesting to note that the increase in the strength of first-order interactions does not have a uniform effect throughout the whole range of σ. In fact, the dependence of C_n or D_n on σ changes sign depending on the magnitude of the latter. Similarly, it is

Table III
Normalized Probabilities from Molecular Dynamics of
g$^+$-η-g$^+$ and g$^+$-η-g$^-$ at O–Si–O–Si

ϕ_{i-1}	ϕ_i	ϕ_{i+1}	normalized probability directly from MD	normalized probability from $P(\eta)$ and $P(\xi\eta)$
g$^+$	g$^-$	g$^+$	0.15	0.16
g$^+$	t	g$^+$	0.50	0.53
g$^+$	g$^+$	g$^+$	0.35	0.31
g$^+$	g$^-$	g$^-$	0.16	0.17
g$^+$	t	g$^-$	0.58	0.54
g$^+$	g$^+$	g$^-$	0.26	0.29

hard to estimate the influence of higher order interactions on the chain conformational behavior, unless systematic analysis in this direction is carried out.

Table III presents the basis for believing that third or higher order interactions might be responsible for d ln $\langle r^2 \rangle_0$/d$T > 0$. This table presents normalized probabilities for triplets in which the first and third bond are both in g$^+$ states or in gauche states of opposite sign. The probabilities listed in the next-to-last column are taken directly from the molecular dynamics trajectory computed in the previous paper.[1] Consequently they are determined by all of the interactions present in the oligomer. The probabilities listed in the last column are those computed from the first- and second-order probabilities deduced from the molecular dynamics trajectory and the assumption that interactions higher than second order are negligible. The probabilities evaluated directly from the molecular dynamics trajectory agree quite well with those calculated from the $P(\eta)$ and $P(\xi\eta)$ when the internal bond in the triplet is in state g$^+$. However, the molecular dynamics trajectory shows a deficiency (excess) of t at the internal bond when its neighbors are gauche placements of the same (opposite) sign. This result implies the influence of third or higher order interactions that are not incorporated in the statistical weight matrices defined in eqs 1 and 2. Neglect of the higher order interactions may be important for d ln $\langle r^2 \rangle_0$/dT if they are strongly dependent on temperature. The high-order interactions can be neglected in the computation of C_n, D_n, and K_x, as shown by the good agreement between experiments and calculations that use eqs 1 and 2.

References and Notes

(1) Bahar, I.; Zuniga, I.; Dodge, R.; Mattice, W. L. *Macromolecules*, preceding paper in the issue.
(2) Flory, P. J.; Crescenzi, V.; Mark, J. E. *J. Am. Chem. Soc.* 1964, *86*, 146.
(3) Flory, P. J. *Statistical Mechanics of Chain Molecules*; Interscience: New York, 1969.
(4) Crescenzi, V.; Flory, P. J. *J. Am. Chem. Soc.* 1964, *86*, 146.
(5) Mark, J. E.; Flory, P. J. *J. Am. Chem. Soc.* 1964, *86*, 138.
(6) Brown, J. F.; Slusarczuk, G. M. *J. Am. Chem. Soc.* 1965, *87*, 931.
(7) Beevers, M. S.; Semlyen, J. A. *Polymer* 1972, *13*, 385.
(8) Scales, L. E.; Semlyen, J. A. *Polymer* 1976, *17*, 601.
(9) Semlyen, J. A. In *Cyclic Polymers*; Semlyen, J. A., Ed.; Elsevier Applied Science Publishers: Essex, U.K., 1986; p 1.
(10) Sutton, C.; Mark, J. E. *J. Am. Chem. Soc.* 1971, *54*, 5011.
(11) Jacobson, H.; Stockmayer, W. H. *J. Chem. Phys.* 1950, *18*, 1600.
(12) Jacobson, H.; Beckmann, C. O.; Stockmayer, W. H. *J. Chem. Phys.* 1950, *18*, 1607.
(13) Flory, P. J. *Macromolecules* 1974, *7*, 383.
(14) Flory, P. J.; Semlyen, J. A. *J. Am. Chem. Soc.* 1966, *88*, 3209.
(15) Flory, P. J.; Suter, U. W.; Mutter, M. *J. Am. Chem. Soc.* 1976, *98*, 5733.
(16) Grigoras, S.; Lane, T. H. *J. Comput. Chem.* 1988, *9*, 25.